Stratospheric solar geoengineering without ozone loss

David W. Keith[a,b,1], Debra K. Weisenstein[a], John A. Dykema[a], and Frank N. Keutsch[a,c]

[a]John A. Paulson School of Engineering and Applied Sciences, Harvard University, Cambridge, MA 02138; [b]John F. Kennedy School of Government, Harvard University, Cambridge, MA 02138; and [c]Department of Chemistry and Chemical Biology, Harvard University, Cambridge, MA 02138

Edited by John H. Seinfeld, California Institute of Technology, Pasadena, CA, and approved November 3, 2016 (received for review September 20, 2016)

Injecting sulfate aerosol into the stratosphere, the most frequently analyzed proposal for solar geoengineering, may reduce some climate risks, but it would also entail new risks, including ozone loss and heating of the lower tropical stratosphere, which, in turn, would increase water vapor concentration causing additional ozone loss and surface warming. We propose a method for stratospheric aerosol climate modification that uses a solid aerosol composed of alkaline metal salts that will convert hydrogen halides and nitric and sulfuric acids into stable salts to enable stratospheric geoengineering while reducing or reversing ozone depletion. Rather than minimizing reactive effects by reducing surface area using high refractive index materials, this method tailors the chemical reactivity. Specifically, we calculate that injection of calcite ($CaCO_3$) aerosol particles might reduce net radiative forcing while simultaneously increasing column ozone toward its preanthropogenic baseline. A radiative forcing of −1 $W{\cdot}m^{-2}$, for example, might be achieved with a simultaneous 3.8% increase in column ozone using 2.1 $Tg{\cdot}y^{-1}$ of 275-nm radius calcite aerosol. Moreover, the radiative heating of the lower stratosphere would be roughly 10-fold less than if that same radiative forcing had been produced using sulfate aerosol. Although solar geoengineering cannot substitute for emissions cuts, it may supplement them by reducing some of the risks of climate change. Further research on this and similar methods could lead to reductions in risks and improved efficacy of solar geoengineering methods.

climate change | geoengineering | stratospheric ozone | climate engineering | atmospheric chemistry

Deliberate introduction of aerosol into the stratosphere, a form of solar geoengineering or Solar Radiation Management (SRM), may reduce impacts of climate change, including regional changes in precipitation and surface temperature (1, 2), by partially and temporarily (3) offsetting radiative forcing from greenhouse gases. The most salient direct risk of sulfate aerosol, the material most commonly proposed for SRM, is stratospheric ozone loss (4, 5). In a 2006 paper (5) that triggered recent interest in SRM, Crutzen suggested that soot particles could warm the polar stratosphere and "thereby hinder the formation of ozone holes." Crutzen's approach rests on manipulating radiative properties to indirectly influence chemistry, whereas here we propose that use of solid aerosol composed of alkaline metal salts that react with hydrogen halides and nitric and sulfuric acid to form stable salts may enable stratospheric SRM while allowing partially independent manipulation of the catalytic reactions that control stratospheric ozone. In contrast to Crutzen's approach, this provides a direct chemical method that may restore ozone concentrations that are reduced by anthropogenic NO_x and halogens while simultaneously providing SRM radiative forcing with minimal stratospheric heating.

Three acids, HNO_3, HCl, and HBr, serve as reservoirs for the nitrogen, NO_x, chlorine, ClO_x, and bromine, BrO_x, radical families that participate in coupled catalytic cycles that destroy ozone. Sulfuric acid, H_2SO_4, can accelerate ozone loss by forming aqueous aerosol that catalyzes reactions such as $HCl + ClONO_2 \rightarrow Cl_2 + HNO_3$, shifting halogens from reservoir species to reactive compounds and altering the NO_x budget via hydrolysis of N_2O_5 to HNO_3. Previous studies found that injection of sufficient SO_2 or particulate sulfate to produce −2 $W{\cdot}m^{-2}$ of radiative forcing—a useful benchmark for SRM—reduced average column ozone by 1 to 13% (2, 6–8).

The use of solid, high refractive index, aerosol particles for SRM was first suggested (9) in the 1990s. That work and most subsequent analyses focused on the mass-specific scattering efficiency, with the implication that solid aerosol might be able to reduce the total mass required for SRM (9–12). In prior work (2), we explored the possibility that solid aerosol might reduce important environmental risks of SRM including (*i*) heating of the lower stratosphere, (*ii*) diffuse scattering of incident sunlight, and (*iii*) ozone loss. Using a model that included the microphysical interactions of solid aerosol with natural background sulfate aerosol, we found that, although some ozone impacts came from reactions such as $HCl + ClONO_2$ on hydrophilic oxide surfaces, the dominant impact was from an increase in sulfuric acid surface as the preexisting background sulfuric acid was distributed over a large surface area of solid particles (2).

Here we consider the possibility of using alkaline (basic) salts of group 1 and 2 metals, such as Na and Ca, to neutralize the acids involved in the catalytic destruction of ozone. These metals might be introduced to the stratosphere in metallic form, as oxides, or as salts formed with weak acids such as carbonic acid. Gas-phase acids will then react to form neutral, solid salts such as NaCl, $Ca(NO_3)_2$, and Na_2SO_4 that are stable in the stratosphere.

Significance

The combination of emissions cuts and solar geoengineering could reduce climate risks in ways that cannot be achieved by emissions cuts alone: It could keep Earth under the 1.5-degree mark agreed at Paris, and it might stop sea level rise this century. However, this promise comes with many risks. Injection of sulfuric acid into the stratosphere, for example, would damage the ozone layer. Injection of calcite (or limestone) particles rather than sulfuric acid could counter ozone loss by neutralizing acids resulting from anthropogenic emissions, acids that contribute to the chemical cycles that destroy stratospheric ozone. Calcite aerosol geoengineering may cool the planet while simultaneously repairing the ozone layer.

Author contributions: D.W.K. conceived the idea; D.W.K., D.K.W., J.A.D., and F.N.K. designed research; F.N.K. developed our treatment of kinetics and interaction between acids; D.W.K., D.K.W., J.A.D., and F.N.K. performed research; D.K.W. performed the chemical-transport modeling experiments; J.A.D. performed the radiative transfer calculations and contributed analysis tools; D.K.W., J.A.D., and F.N.K. analyzed data; and D.W.K., D.K.W., J.A.D., and F.N.K. wrote the paper.

The authors declare no conflict of interest.

This article is a PNAS Direct Submission.

Freely available online through the PNAS open access option.

[1]To whom correspondence should be addressed. Email: david_keith@harvard.edu.

This article contains supporting information online at www.pnas.org/lookup/suppl/doi:10.1073/pnas.1615572113/-/DCSupplemental.

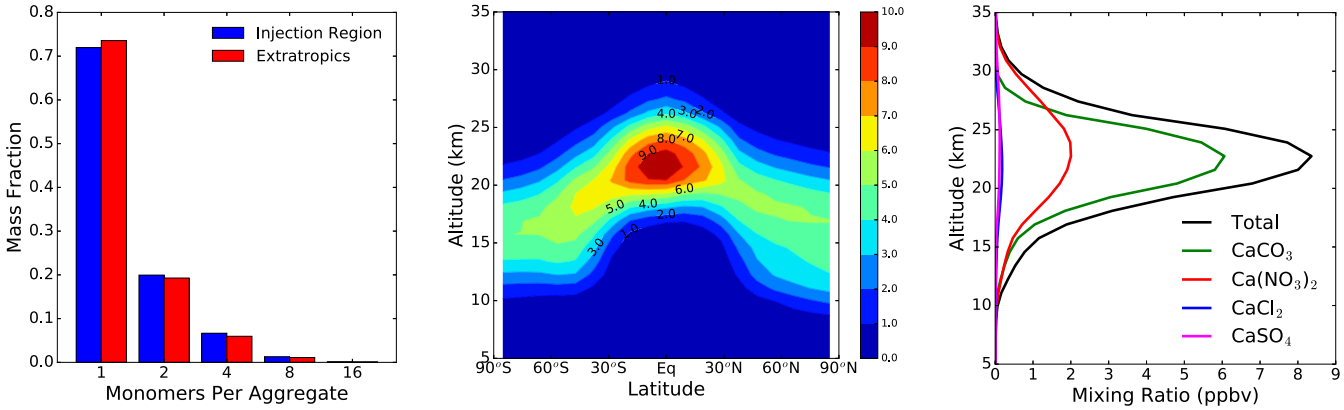

Fig. 1. Particle aggregation, spatial distribution and chemistry. All plots represent annual average conditions resulting from a 5.6-Tg·y^{-1} steady-state injection of calcite. (*Left*) The fraction of solid particle mass per sectional bin vs. number of monomers in the fractal aggregate. (*Middle*) Particle number density (cm^{-3}) as a function of latitude and altitude. (*Right*) Composition of solid particles resulting from reaction with acids showing total (black line) and $CaCO_3$, $CaCl_2$, $Ca(NO_3)_2$, and $CaSO_4$ mixing ratios (parts per billion by volume) averaged from 60°S to 60°N.

The surfaces of these salts have low rates for acid-catalyzed reactions, as they are neutral, and do not contribute to bulk hydrolysis reactions, as they are solid.

Particles composed of, or coated with, alkaline compounds might reduce ozone loss through reaction with the background sulfate aerosol or reaction with gas-phase acids. The rate of the first mechanism depends on the flux of H_2SO_4 onto particles by coalescence or condensation. The liquid–solid reaction will rapidly neutralize the acid to form a dry salt if there is sufficient base. The rate of the second mechanism will depend on the kinetics of the gas–solid reactions.

As a specific example, we model the use of calcite ($CaCO_3$) aerosol for SRM using an extension of the model we developed for solid aerosols such as alumina and diamond (2). We simulate a monodisperse 275-nm-radius calcite aerosol injected uniformly between 20 km and 25 km altitude within 30 degrees of the equator. We use a 2D chemical transport and aerosol microphysics model that includes a prognostic size distribution for three categories of aerosol: liquid aerosol, solid aerosol, and liquid-coated solid aerosol (*Methods*). As we mention in *Discussion*, however, many of the rate constants have significant uncertainty. Radiative forcing is computed using a high-resolution band model (*Methods*).

Results

Sulfate aerosol warms the lower stratosphere, which would likely increase the flux of water vapor through the tropical tropopause. Once in the stratosphere, the additional water vapor can accelerate ozone loss and will add to the radiative forcing of climate, offsetting some of the intended benefit of adding the sulfates. Heating of the lower stratosphere is therefore a significant contributor to the risks of sulfate aerosol SRM. Calcite may reduce these risks because it causes less warming than either sulfates or solids such as titania or alumina that have been analyzed elsewhere (12–17). A high-accuracy radiative calculation using a column model with fixed dynamical heating shows that for a −2-W·m^{-2} radiative forcing using optimally sized particles, sulfate warms the lower stratosphere by 2.4 K, whereas warming is only 0.2 K for calcite (18).

The extent to which acids will react with calcite and be neutralized as calcium salts depends on their relative abundance, acidity, and vapor pressure. Although H_2SO_4 is the weakest of the four acids, formation of $CaSO_4$ is favored due to the low vapor pressure of sulfuric acid, so H_2SO_4 aerosol will react with $Ca(NO_3)_2$ to release HNO_3 gas unless unreacted calcite remains. A similar competition exists between HNO_3 and HCl, with formation of $Ca(NO_3)_2$ being favored over $CaCl_2$ due to the high vapor pressure of HCl. At low calcite loadings, the coagulation process with sulfuric acid aerosol will therefore reduce the effectiveness of removing gas-phase HNO_3 and HCl. However, the resulting solid, nonacidic $CaSO_4$ surfaces have much lower catalytic activity than liquid sulfuric acid aerosol for acid-catalyzed and liquid-phase reactions.

Fig. 1 shows the extent of particle aggregation along with the spatial distribution and composition of solid particles for a calcite injection rate of 5.6 Tg·y^{-1}, the maximum injection rate we studied, which was chosen to produce approximately −2 W·m^{-2} of global average radiative forcing. The concentration of solid particles in the lower stratosphere ranges from about 4 cm^{-3} to 8 cm^{-3}, and only about a third of the solid aerosol coalesces into aggregates. The dominant salt formed is $Ca(NO_3)_2$, consistent with the greater stratospheric abundance of HNO_3 relative to HCl, HBr, and H_2SO_4. Fig. 2 shows the resulting changes in the individual catalytic cycles and the ozone distribution. The largest impact is the reduction in NO_x in the lower stratosphere. The decrease in NO_x shifts the halogens from reservoir species to ClO_x and BrO_x, which increases their relative importance along with the HO_x cycle (Fig. 2, *Left*), but, because HCl and HBr are also removed by reaction with calcite, the overall impact is nevertheless a decrease in ozone loss rate. In addition, ozone destruction via the NO_x catalytic cycle is greatly reduced below 35 km. Annual average column ozone is increased by 6.4%, although ozone concentration decreases in the lowermost stratosphere and upper troposphere. Figs. S1 and S2 show similar results for smaller injection rates.

The resulting trade-off between radiative forcing and ozone loss is shown in Fig. 3 for a range of calcite injection rates. Note the strong nonlinearity in the ozone response to injection rates that arises, in part, from the competition between HNO_3, HCl, and H_2SO_4 as the amount of $CaCO_3$ is increased (Figs. S3 and S4). The response for calcite may be compared with prior results for sulfate, alumina, and diamond, which all reduce column ozone. As a crude sensitivity test, we scaled all of the gas–solid reaction rates from 10^{-1} to 10^{-4} and found that the column response (also shown in Fig. 3) is surprisingly robust although the dominant mechanism and vertical distributions of ozone change shift considerably (Fig. S4).

Discussion

We note the conceptual similarities between our alkali addition and Cicerone et al.'s 1991 proposal (19) to add propane to the Antarctic polar vortex to limit ozone loss by converting ClO_x into

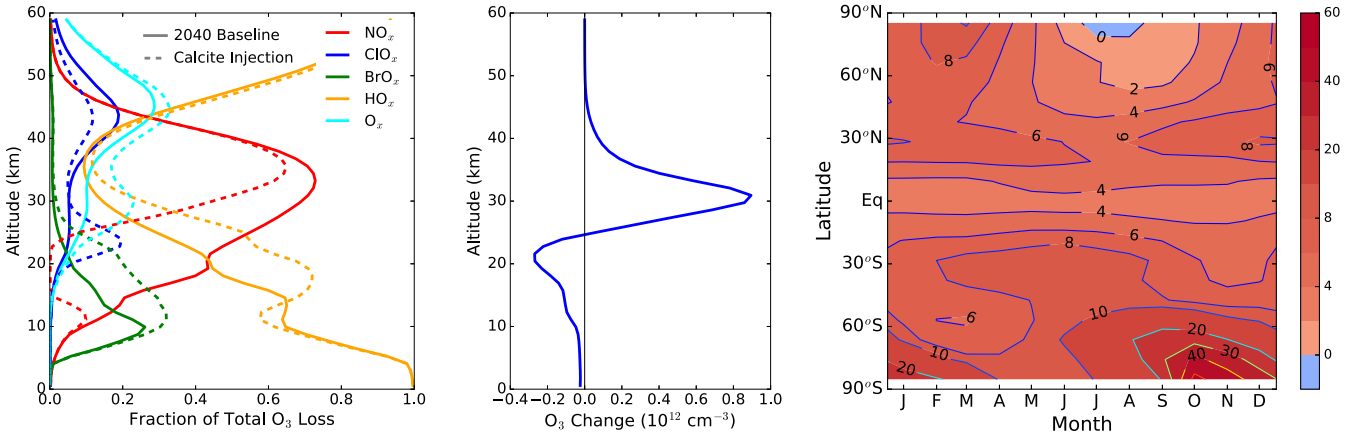

Fig. 2. Changes in ozone chemistry and distribution. All plots show changes resulting from a 5.6-Tg·y^{-1} steady-state injection of calcite. (*Left*) Fraction of ozone loss caused by various catalytic cycles as a function of altitude, averaged from 60°S to 60°N for annual average conditions (see Table S1 for definitions of the catalytic cycles). (*Middle*) Annual average change in ozone (10^{12} molecules cm^{-3}) as a function of latitude and altitude. (*Right*) Change in column ozone (percent) as a function of latitude and season.

HCl, a proposal that was later found to have ignored a crucial HO_x feedback. We cannot discount the possibility that we too have ignored some crucial feedback. Our specific numerical results depend on uncertain assumptions. Perhaps most importantly, the gas–solid reaction rates for many of the neutralization reactions are not known, especially under stratospheric conditions. We assume that the entire particle is available for reaction, with rates declining linearly to zero in proportion to the fraction of remaining reactant, e.g., $CaCO_3$/Ca, but we do not know how uptake/neutralization rates change as calcite surfaces are transformed to salt coatings, although the range of gammas we explore, 1.0 to 10^{-4}, encompasses the range of observations (20). Finally, the rate constants for heterogeneous halogen-activating reactions (e.g., HCl + $ClONO_2$) are not known for the (mixed) salt surfaces, and refractive indices for such particles have not been measured. Nor do we know if the photochemistry of mixed $Ca(NO_3)_2$/$CaCO_3$ particles is relevant.

Notwithstanding these uncertainties, we suggest that there is a nontrivial possibility that use of $CaCO_3$, or a hybrid approach that employs reactive alkali metal salts in combination with high refractive index solid aerosol, could have significantly less environmental risk than sulfate aerosol for a given level of radiative forcing. We therefore suggest that research on stratospheric aerosol SRM needs to move beyond an exclusive focus on sulfate.

Any practical application of this idea should not, of course, proceed until uncertainties about the science and governance are substantially resolved. However, future effort to assess calcite aerosol for SRM is, in part, contingent on judgments about feasibility of implementation. Although analysis of the feasibility is far beyond the scope of this study, we note that (*i*) submicron calcite particles are available commercially, (*ii*) methods of preparing monodisperse calcite exist (21), and (*iii*) engineering studies have demonstrated that teragrams per year of material can be lofted to the lower stratosphere with relatively low cost and technical risk (22). The most obvious engineering unknown would seem to be the ability to disperse solid particles while avoiding agglomeration.

Calcium delivered to the stratosphere will eventually return to the surface, so further consideration of this idea must include studies of the environmental risks of calcium aerosol in the troposphere or its biological impact once deposited on the surface. Calcium is an important component in windblown aerosol "dust," so a comparison of fluxes provides some indication of the impact of stratospheric Ca on the chemistry of the lower atmosphere and surface. A flux of 5.6 Tg·y^{-1} $CaCO_3$, the largest value analyzed, corresponds to a global average Ca deposition rate of 0.005 g·m^{-2}·y^{-1}. In comparison, the lowest estimate of Ca deposition by Aeolian dust in areas remote from dust sources is of order 0.01 g·m^{-2}·y^{-1}, though deposition rates exceed 1 g Ca·m^{-2}·y^{-1} over large areas of the continental land surface (23). In addition, speciation of the stratospheric nitrate transported to the surface will be shifted from HNO_3 toward $Ca(NO_3)_2$, which may have consequences on rainwater acidity and nitrate bioavailablity.

Previous work has shown that solid aerosol can enable SRM with less heating of the lower stratosphere (18) and less ozone loss than sulfates, and that high refractive index particles such as alumina or diamond have lower forward scattering (2). Our work suggests that solid alkali aerosol might significantly reduce the risks of SRM compared with the use of sulfate to produce the same radiative forcing. The combination of solid high-index aerosol with alkali coatings or separate alkali aerosol might allow partially independent manipulation of radiative forcing and stratospheric chemistry and heating. In addition to reversing ozone loss caused by historical chlorofluorocarbon emissions, the injection of alkalis may provide a method to counter the steady growth of stratospheric NO_x caused by anthropogenic N_2O emissions (24). Laboratory and small-scale field experiments (using <1 kg of materials) (25) are, however, essential to reduce uncertainties in heterogeneous reaction rates and photochemistry of mixed salt aerosol, which are critical to predicting stratospheric ozone loss rates.

Materials and Methods

Chemical Transport Model. We use the AER 2-D chemical transport–aerosol model (26–28), as modified to include both liquid sulfate particles and solid particles along with their interactions (2). The model uses a sectional representation of aerosol size distributions, with 40 logarithmically spaced bins for sulfate particles and eight bins for solid particles. Calcite particles are treated the same as alumina particles, forming fractal aggregates upon coagulation. We use a monomer radius of 275 nm and take the fractal dimension D_f to be 2.1 (29). Compared with the alumina particles of 240 nm radius studied in Weisenstein et al. (2), pure calcite particles in this study sediment about 15% slower due to their larger radius but lower density of 2.7 g·cm^{-3}.

We simulate emission of monodisperse calcite particles of 275 nm radius, selecting this radius for optimal radiative properties (18). Emissions are uniform in time and space between 30°S and 30°N and 20 km to 25 km altitude at rates of 0.3, 1, 2.8, and 5.6 Tg·y^{-1}. Our calculations represent the 2040 atmosphere, with halogen and trace gas concentrations under representative concentration pathway (RCP) 6.0 (30) The model transport and temperature fields are prescribed to the 1978–2004 climatology (31) and are

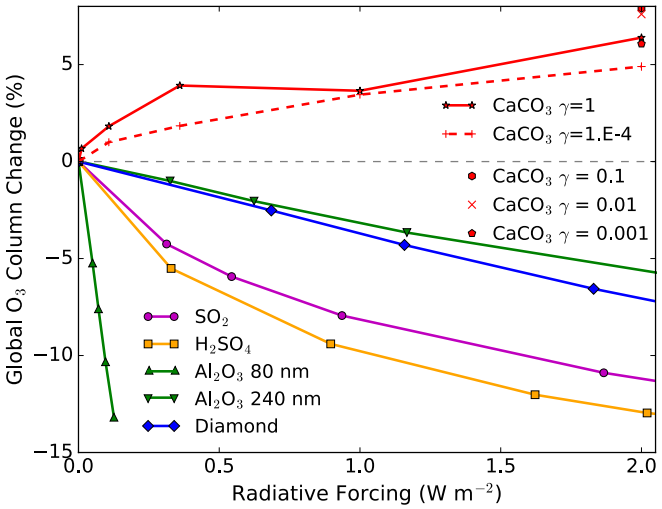

Fig. 3. Trade-off between ozone loss and radiative forcing from geoengineering. Change in annual average global column ozone is plotted versus the computed aerosol radiative forcing. Changes in ozone are computed with respect to a 2040 baseline. Positive values represent an increase in ozone. Results for calcite injection rates ranging from 0.3 Tg·y^{-1} to 5.6 Tg·y^{-1} shown (red line and symbols) where the gas–solid reaction rates, γ, are varied to explore parameter uncertainty. For comparison, we show prior results for injection of alumina, diamond, and sulfate, either from injection of gas-phase SO_2 or sulfuric acid (2).

repeated annually. Chemistry and aerosol are interactive via the sulfur source gases and heterogeneous reactions affecting ozone concentration, as described in Weisenstein et al. (2). We integrate model calculations for about 10 y, to an annually repeating condition, and analyze results from the final year.

Calcite Chemistry. Because $CaCO_3$ is basic (alkaline), it is expected to react with gas-phase acid species such as HCl and HNO_3 in the stratosphere, forming solid salts of $CaCl_2$ and $Ca(NO_3)_2$; this will modify the composition of the solid particles while removing chlorine and nitrogen from the gas phase. Our model is not equipped to handle multicomponent solid particles and their interaction with gases, but we can easily model gas-phase interactions on a surface and assign a sedimentation rate to the resulting salts. Therefore, we added five pseudogas-phase compounds $CaCO_3$, $CaCl_2$, $CaBr_2$, $Ca(NO_3)_2$, and $CaSO_4$, to the model and applied sedimentation velocities obtained as the mass-weighted average over the solid particle bin sizes. The model injects the pseudogas $CaCO_3$ at the same rate as particulate $CaCO_3$, so we can track the unreacted fraction. The following additional reactions are added to the model:

$$2\ HCl + CaCO_3 \rightarrow CaCl_2 + CO_2 + H_2O \quad [1]$$

$$2\ HBr + CaCO_3 \rightarrow CaBr_2 + CO_2 + H_2O \quad [2]$$

$$2\ HNO_3 + CaCO_3 \rightarrow Ca(NO_3)_2 + CO_2 + H_2O \quad [3]$$

$$H_2SO_4 + CaCO_3 \rightarrow CaSO_4 + CO_2 + H_2O, \quad [4]$$

where here and in Eqs. **6**–**10**, all of the Ca-containing species are in solid phase and all other species are gas phase. These reactions result in HCl, HBr, HNO_3, and H_2SO_4 being removed from the stratosphere, decreasing the concentrations of Cl_y, Br_y, NO_y, and H_2SO_4. We assume that reaction probabilities (γ) for reactions **1**–**4** are 1.0 (we vary this assumption as a sensitivity test) and that their reaction rates, R_i, depend on the surface area density (S_p) of the solid $CaCO_3$ particles as well as the reaction probability (γ_i) and the thermal speed (v_g) of the gas-phase reactant.

$$R_i = \gamma_i F_p S_p \frac{v_g}{4}[G], \quad [5]$$

where [G] is the concentration of the gas-phase reactant in molecules per cubic centimeter and F_p is the fraction of the total Ca as $CaCO_3$, assuming that the full particle volume may react with acidic species, not the surface layer alone. Goodman et al. (32) reported such behavior for the reaction of calcite with HNO_3 at a relative humidity of 20%. However, the system has not been studied under stratospheric condition with respect to T and RH, although it has been shown that reactions of HNO_3 with solids are faster in the presence of UV radiation (33). In this work, we scale the rate linearly to zero, via factor F_p, as the unreacted calcite is used up.

In addition, we assume that coagulation between solid $CaCO_3$ particles and liquid sulfate particles, or condensation of gas-phase H_2SO_4 onto $CaCO_3$ particles, results in formation of solid $CaSO_4$, as in reaction **4**. Because H_2SO_4 has a much lower volatility in the stratosphere than HCl and HNO_3, we make the further assumption that, if all $CaCO_3$ has been reacted but H_2SO_4 remains as a liquid on the particles, then the chlorine in $CaCl_2$ or the nitrate in $Ca(NO_3)_2$ can be displaced by sulfate, liberating gas-phase HCl or HNO_3. These reactions between liquid sulfate and solid calcite or calcite salts are assumed instantaneous. Similar gas-phase reactions of H_2SO_4 and HNO_3 may displace $CaCl_2$ or $Ca(NO_3)_2$ from the solid particles (reactions **6**–**8**). Reactions of $ClONO_2$ and $BrONO_2$ are also likely to displace $CaCl_2$ in favor of $Ca(NO_3)_2$, in this case producing the gas-phase products Cl_2 and BrCl, which would rapidly decompose into ozone-destroying monatomic Cl and Br (reactions **9** and **10**). Again, we assume reaction probabilities of 1.0, which are likely overestimates. The additional gas–solid reactions are

$$H_2SO_4 + CaCl_2 \rightarrow CaSO_4 + 2\ HCl \quad [6]$$

$$2\ HNO_3 + CaCl_2 \rightarrow Ca(NO_3)_2 + 2\ HCl \quad [7]$$

$$H_2SO_4 + Ca(NO_3)_2 \rightarrow CaSO_4 + 2\ HNO_3 \quad [8]$$

$$2\ ClONO_2 + CaCl_2 \rightarrow Ca(NO_3)_2 + 2\ Cl_2 \quad [9]$$

$$2\ BrONO_2 + CaCl_2 \rightarrow Ca(NO3)_2 + 2\ BrCl, \quad [10]$$

where the reaction rates follow Eq. **5**, except that F_p is the fraction of the total Ca as solid reactant, either $CaCl_2$ or $Ca(NO_3)_2$.

The treatment we have adopted of the solid salt components produced by reactions with calcite particles allows us to avoid modeling five components of the solid particles in each of eight size bins. Here we assume the same composition for all eight size bins and use the fractions of $CaCO_3$ and derived salts in the reaction rate calculations. See Fig. S3 for the calcite particle composition as a function of injection rate. We find that the pseudogas-phase calcium species have a 9% larger stratospheric burden than the solid species, providing a rough estimate of the error committed by our use of the pseudogas species approximation.

Mechanisms of Ozone Change. The consequences of reactions **1**–**3** are to remove chlorine, bromine, and nitrogen oxide gases from the stratosphere and convert them into solid salts that would not participate in catalytic reactions destroying ozone. The solid salts would be removed from the stratosphere by sedimentation and advective transport and subsequently removed from the troposphere by cloud processes and deposition. For an injection of 5.6 Tg·y^{-1} of $CaCO_3$, we find that the stratospheric burdens of gaseous Cl_y, Br_y, and NO_y decrease by 77%, 4%, and 77%, respectively. In the lower stratosphere, Cl_y and NO_y decrease by over 90% (Fig. S4). The liquid sulfate surface area density of the stratosphere also decreases, because any sulfate that contacts the calcite particles is converted to the stable salt $CaSO_4$. Thus, the surface area for heterogeneous reactions that convert reservoir ClO_x and NO_x to active radical forms is reduced, and the surface of the calcite particles is unlikely to participate in catalytic reactions as long as the unreacted $CaCO_3$ exceeds the adsorbed liquid acid. Table S1 lists the rate-limiting reactions of the ozone loss cycles important in the extrapolar stratosphere, and includes reactions **9** and **10** above.

Radiative Transfer Calculations. Radiative transfer calculations are performed in this study using the Rapid Radiative Transfer Model (RRTM) (34, 35) including absorption and scattering processes for 16 streams. RRTM separates shortwave and longwave calculations into two separate programs, spanning 820 cm^{-1} to 50,000 cm^{-1} in 14 bands and 10 cm^{-1} to 3,250 cm^{-1} in 19 bands. Fluxes are computed via the delta-Eddington approximation. The diurnal variability in the shortwave radiative calculations is taken into account by computing radiative quantities at 10 solar zenith angles, and averaging to compute the daily mean. Aerosol scattering parameters are calculated using tabulated complex refractive index data for calcite (36, 37) within a fractal scattering framework (38). Further details are found in Dykema et al. (18).

ACKNOWLEDGMENTS. This work was funded by the Fund for Innovative Climate and Engineering Research and the Star Family Challenge for Promising Scientific Research.

1. Kravitz B, et al. (2014) A multi-model assessment of regional climate disparities caused by solar geoengineering. *Environ Res Lett* 9(7):074013.
2. Weisenstein DK, Keith DW, Dykema J (2015) Solar geoengineering using solid aerosol in the stratosphere. *Atmos Chem Phys* 15(20):11835–11859.
3. Keith DW, MacMartin DG (2015) A temporary, moderate and responsive scenario for solar geoengineering. *Nat Clim Change* 5(3):201–206.
4. National Research Council (2015) *Climate Intervention: Reflecting Sunlight to Cool Earth* (Natl Acad Press, Washington, DC).
5. Crutzen PJ (2006) Albedo enhancement by stratospheric sulfur injections: A contribution to resolve a policy dilemma? *Clim Change* 77(3):211–220.
6. Heckendorn P, et al. (2009) The impact of geoengineering aerosols on stratospheric temperature and ozone. *Environ Res Lett* 4(4):045108.
7. Pitari G, et al. (2014) Stratospheric ozone response to sulfate geoengineering: Results from the Geoengineering Model Intercomparison Project (GeoMIP). *J Geophys Res Atmos* 119(5):2629–2653.
8. Tilmes S, Müller R, Salawitch R (2008) The sensitivity of polar ozone depletion to proposed geoengineering schemes. *Science* 320(5880):1201–1204.
9. Teller E, Wood L, Hyde R (1997) *Global Warming and Ice Ages: I. Prospects for Physics-Based Modulation of Global Change* (Lawrence Livermore Natl Lab, Livermore, CA).
10. Blackstock J, Battisti D, Caldeira K (2009) *Climate Engineering Responses to Climate Emergencies* (Novim Study Group, Santa Barbara, CA).
11. Keith DW (2010) Photophoretic levitation of engineered aerosols for geoengineering. *Proc Natl Acad Sci USA* 107(38):16428–16431.
12. Pope F, et al. (2012) Stratospheric aerosol particles and solar-radiation management. *Nat Clim Change* 2(10):713–719.
13. Benduhn F, Lawrence M (2013) An investigation of the role of sedimentation for stratospheric solar radiation management. *J Geophys Res Atmos* 118(14):7905–7921.
14. Maruyama S, Nagayama T, Gonome H, Okajima J (2015) Possibility for controlling global warming by launching nanoparticles into the stratosphere. *J Thern Sci Tech-Jpn* 10(2):JTST0022.
15. Committee on Science Engineering and Public Policy (1992) Appendix Q: Geoengineering options. *Policy Implications of Greenhouse Warming: Mitigation, Adaptation, and the Science Base* (Natl Acad Press, Washington, DC), pp 817–835.
16. Ferraro AJ, Highwood EJ, Charlton-Perez AJ (2011) Stratospheric heating by potential geoengineering aerosols. *Geophys Res Lett* 38(24):L24706.
17. Jones AC, Haywood JM (2016) Climatic impacts of stratospheric geoengineering with sulfate, black carbon and titania injection. *Atmos Chem Phys* 16(5):2843–2862.
18. Dykema JA, Keith DW, Keutsch FN (2016) Improved aerosol radiative properties as a foundation for solar geoengineering risk assessment. *Geophys Res Lett* 43(14): 7758–7766.
19. Cicerone RJ, Elliott S, Turco RP (1991) Reduced antarctic ozone depletions in a model with hydrocarbon injections. *Science* 254(5035):1191–1194.
20. Santschi Ch, Rossi MJ (2006) Uptake of CO_2, SO_2, HNO_3 and HCl on calcite ($CaCO_3$) at 300 K: Mechanism and the role of adsorbed water. *J Phys Chem A* 110(21):6789–6802.
21. Atchudan R, Na HB, Cheong IW, Jool J (2015) Facile synthesis of monodispersed cubic and spherical calcite nanoparticles in the presence of cetyltrimethylammonium bromide. *J Nanosci Nanotechnol* 15(4):2702–2714.
22. McClellan J, Keith DW, Apt J (2012) Cost analysis of stratospheric albedo modification delivery systems. *Environ Res Lett* 7(3):034019.
23. Lawrence CR, Neff JC (2009) The contemporary physical and chemical flux of aeolian dust: A synthesis of direct measurements of dust deposition. *Chem Geol* 267(1):46–63.
24. Portmann RW, Daniel JS, Ravishankara AR (2012) Stratospheric ozone depletion due to nitrous oxide: Influences of other gases. *Philos Trans R Soc Lond B Biol Sci* 367(1593):1256–1264.
25. Dykema JA, Keith DW, Anderson JG, Weisenstein D (2014) Stratospheric controlled perturbation experiment: a small-scale experiment to improve understanding of the risks of solar geoengineering. *Philos Trans R Soc Lond A Phys Eng Sci* 372(2031): 20140059.
26. Weisenstein D, Penner J, Herzog M, Liu X (2007) Global 2-D intercomparison of sectional and modal aerosol modules. *Atmos Chem Phys* 7(9):2339–2355.
27. Weisenstein DK, et al. (2004) Separating chemistry and transport effects in two-dimensional models. *J Geophys Res Atmos* 109(D18):D18310.
28. Weisenstein DK, et al. (1997) A two-dimensional model of sulfur species and aerosols. *J Geophys Res Atmos* 102(D11):13019–13035.
29. Farin D, Avnir D (1987) Reactive fractal surfaces. *J Phys Chem* 91(22):5517–5521.
30. Hijioka Y, Matsuoka Y, Nishimoto H, Masui T, Kainuma M (2008) Global GHG emission scenarios under GHG concentration stabilization targets. *J Global Environ Eng* 13: 97–108.
31. Fleming EL, Jackman CH, Stolarski RS, Considine DB (1999) Simulation of stratospheric tracers using an improved empirically based two-dimensional model transport formulation. *J Geophys Res Atmos* 104(D19):23911–23934.
32. Goodman A, Underwood G, Grassian V (2000) A laboratory study of the heterogeneous reaction of nitric acid on calcium carbonate particles. *J Geophys Res Atmos* 105 (D23):29053–29064.
33. Usher CR, Michel AE, Grassian VH (2003) Reactions on mineral dust. *Chem Rev* 103(12): 4883–4940.
34. Clough SA, et al. (2005) Atmospheric radiative transfer modeling: A summary of the AER codes. *J Quant Spectrosc Radiat Transfer* 91(2):233–244.
35. Mlawer EJ, Taubman SJ, Brown PD, Iacono MJ, Clough SA (1997) Radiative transfer for inhomogeneous atmospheres: RRTM, a validated correlated-k model for the longwave. *J Geophys Res Atmos* 102(D14):16663–16682.
36. Ghosh G (1999) Dispersion-equation coefficients for the refractive index and birefringence of calcite and quartz crystals. *Opt Commun* 163(1):95–102.
37. Long L, Querry M, Bell R, Alexander R (1993) Optical properties of calcite and gypsum in crystalline and powdered form in the infrared and far-infrared. *Infrared Phys* 34(2): 191–201.
38. Rannou P, McKay C, Botet R, Cabane M (1999) Semi-empirical model of absorption and scattering by isotropic fractal aggregates of spheres. *Planet Space Sci* 47(3): 385–396.